TID-28556

MASTER

ADVANCED THERMIONIC ENERGY CONVERSION

ERDA CONTRACT EY-76-C-02-2263
NASA CONTRACT NAS3-20303

JOINT HIGHLIGHTS AND STATUS REPORT

JANUARY, FEBRUARY 1978

PREPARED BY

RASOR ASSOCIATES, INCORPORATED
253 HUMBOLDT COURT
SUNNYVALE, CALIFORNIA 94086

DISCLAIMER

Task 3 - Converter Electrode Technology

1320 - Negative Ion Effects (L.K. Hansen)

As described last month, the complexity of the negative ion data acquired with both the research converter and quadrupole negative ion test station has prompted a more detailed analysis of space charge limited diode operation. The analysis begun last month continued during this report period. A computer program has been written based on this analysis which will calculate the I-V characteristic for a general space charge diode. At present the program is written to include the emission of electrons and negative ions from only one electrode, but the calculations are done in such a way that generalization to include positive ions and electron emission from the other electrode is straight-forward.

The quadrupole negative ion test station has been reassembled after the move. It will now be put back into operation to further study the negative ion characteristics determined to date. It will then be modified to permit more precise measurements over a broader range of cesium pressures and electrode temperatures.

Task 4 - Advanced Converter Technology

1410 - Converter Performance Evaluation

Negative Ion Converter Tests (M.L. Manda) - As discussed last month, the objective of this task is to improve converter performance by reducing the production rate of negative ions associated with the presence of hydrogen. The procurement phase of this activity was begun during this reporting period. A 400 l/sec noble VacIon pump has been received and is being incorporated into a test stand. Other major test stand components such as feedthroughs and power supplies have also been received. The belljar is being fabricated and should be completed during the next reporting period. The molybdenum electrode substrates have been prepared and are currently having W(110) deposited on them. This activity should be completed in about one month.

Fabrication of the cesium delivery and hydrogen removal systems has begun. Test brazes joining copper directly to titanium have been performed.

Initial designs for a palladium window have indicated a need for tests to determine if palladium can be joined to kovar. Information obtained from the literature indicates that there may be difficulties in making this particular joint.

Activity in this task will decrease during the next few months as other tasks take priority. The effort will be resumed in June with testing anticipated in August.

Structured Electrode Tests (G.L. Hatch) - The first in a series of structured electrode converters was fabricated during this period. The converter, the 3rd in the series of standard "SC" planar electrode devices, uses both an unstructured molybdenum emitter and unstructured molybdenum collector. It will serve to provide the first set of reference performance curves against which the performance of future structured devices will be compared. Molybdenum was selected for the electrode material to minimize the effect of varying electrode work functions as different structures are tested. Surfaces such as tungsten would provide higher, but less reproducible levels of performance.

The converter is being installed in its test stand. A modification in the collector and cesium reservoir designs to permit greater testing flexibility has required changes in the test stand instrumentation. These changes should be completed soon and testing started in March.

The next two converters in the test series will use structured molybdenum collectors. The first of these will have an area ratio of four. It consists of parallel grooves 6 mils wide and 18 mils deep separated by 6 mil wide lands. The grooves were cut using an abrasive wheel. The second structured collector has an area ratio of three. It also has parallel grooves which have been EDM'd, each 6 mils wide, 12 mils deep, and separated by 6 mil lands. Fabrications of both collectors is complete and converter fabrication is in process.

1420 - Converter Structure

Off-the-shelf Envelope Converter (OSEC) (N.S. Rasor) - The pilot model OSEC has been operated in air at a variety of operating points for

about 20 hours and remains fully operational. Fig. 1 shows an ignited and unignited I-V characteristic for near-optimum operation at T_E = 1535°K.

The primary purpose of the pilot model was to establish the integrity of specific off-the-shelf electron tube components when used as a cesium vapor converter envelope operating in air. The use of a nickel emitter limited the emitter temperature to less than about 1600°K, and no means was provided for direct measurement of emitter temperature.

Evaporation of braze material from point A in Fig. 2 during welding of the emitter to the feedthrough assembly caused a low resistance path over the inner surface B of the emitter-EB heater insulator. This imposed two significant constraints on subsequent operation of the pilot model. First, the emission current from the emitter to the EB filament could not be used to determine the emitter temperature as planned. Second, the EB voltage was limited to less than 100 volts due to breakdown over the insulator surface at higher voltage. This required more than 75% of the input power to be by radiation from the filament. In addition to severely limiting the available heat input, it also caused leakage of much input energy from the emitter cavity which tended to overheat the feedthrough assembly and otherwise upset the design temperature balance of the diode envelope.

This problem is corrected in the new models under construction by machining away the brazed component and redesigning the emitter weld joint, as shown in Fig. 2. As an additional precaution, a tantalum getter ring is inserted at C to shadow the insulator from any other evaporation products.

Other than these readily-correctable difficulties, the diode performed satisfactorily and typically. The ignited characteristic (Fig. 1a) shows some evidence of end effects, which are typical of cylindrical converters. Emitter temperatures were inferred from the unignited mode saturation current J_a. Emitter work functions inferred from this T_E and the ignited mode saturation current indicated a bare work function of $\phi_o \simeq 4.8$- 5.0 eV. As the cesium pressure was decreased, the ignition tail would disappear when expected. A barrier index of 2.1 eV was obtained at T_C/T_R = 1.6 and pd = 10 mils-torr. Stable and reproducible operation was obtained throughout the tests.

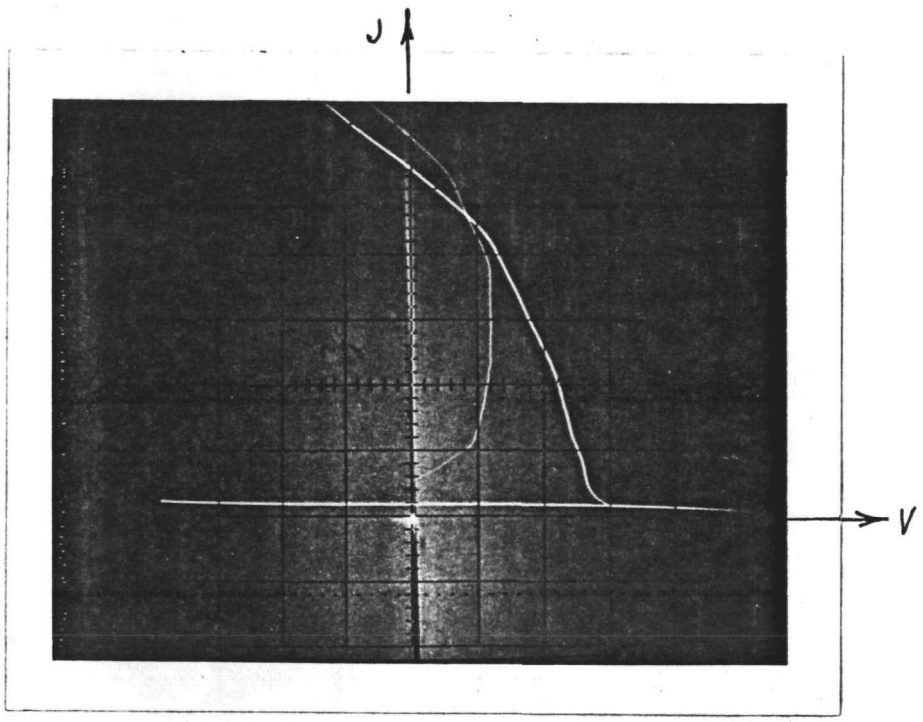

Fig. 1a OSEC Pilot Model Ignited I-V Characteristic (vert. 5 amp/div; horiz. 0.2 v/div.; T_E = 1535°K, T_C = 820 °K, T_R = 523 °K, d = 20 mils, A_E = 9.3 cm^2).

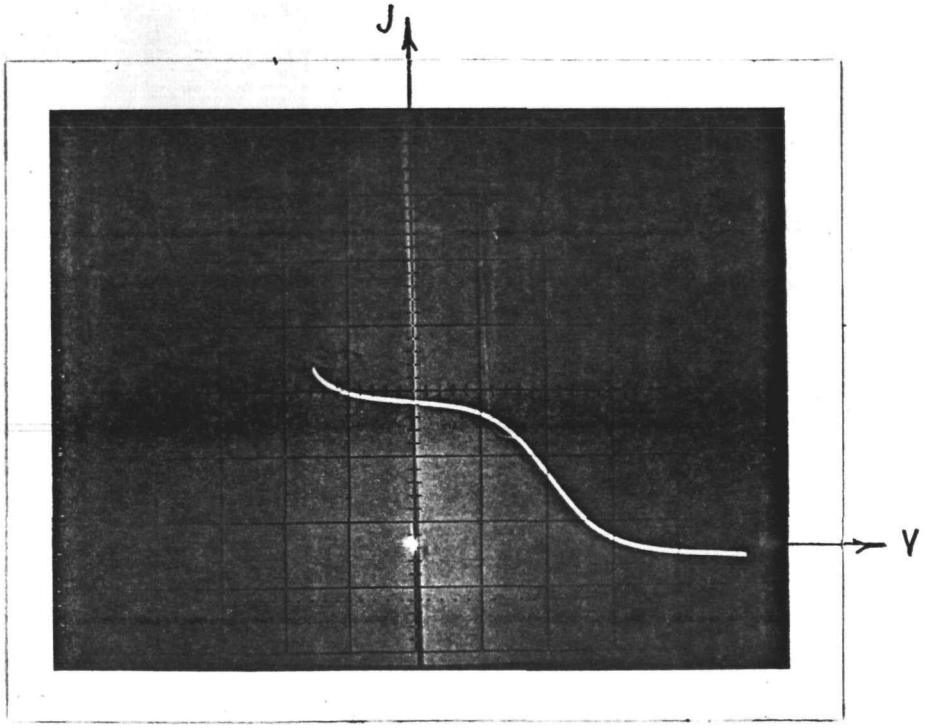

Fig. 1b OSEC Pilot Model Unignited JV Characteristic (vert. 0.5 amp/div.; horiz. 0.5 v/div;otherwise as in Fig. 1a).

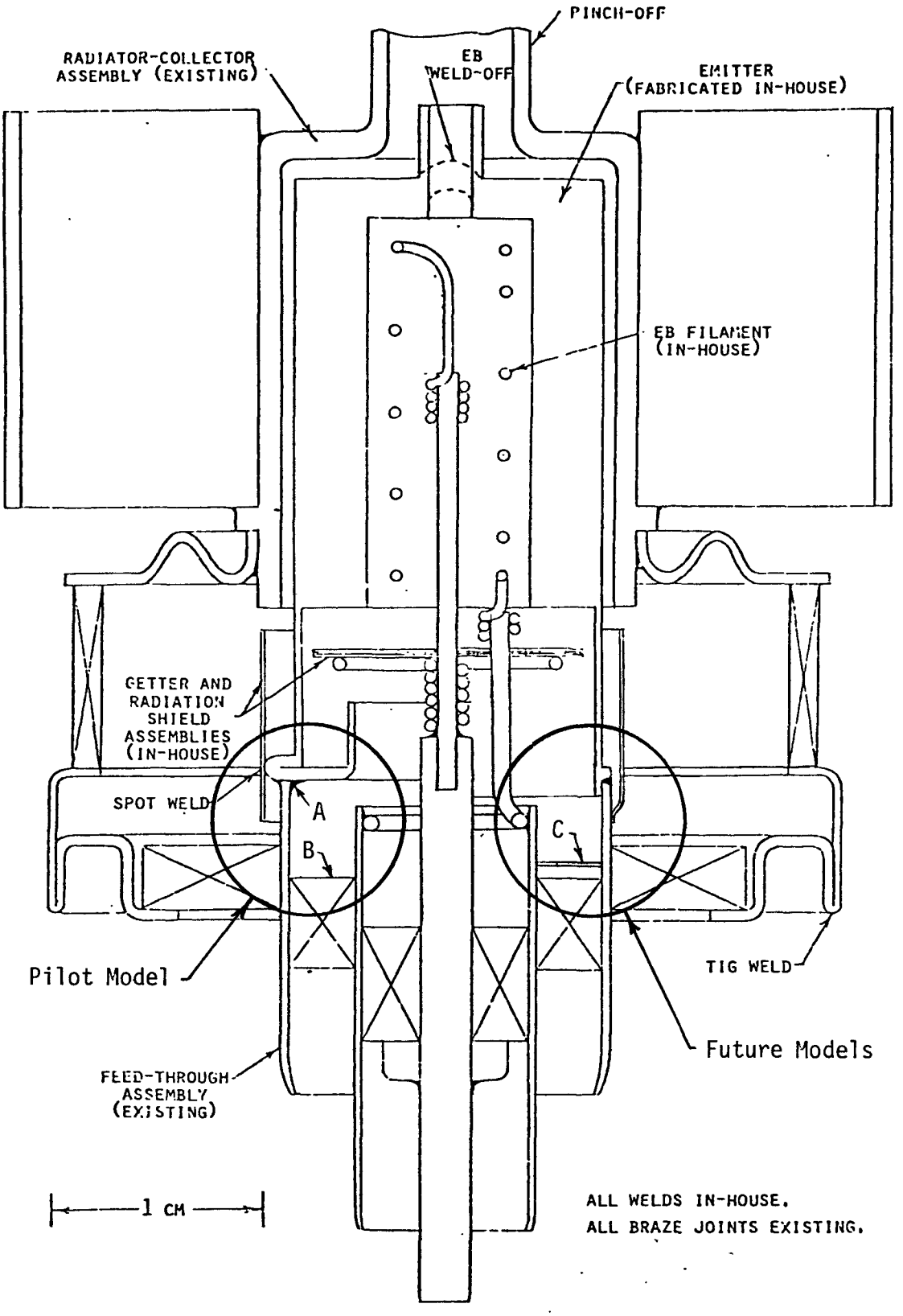

Fig. 2 Section Drawing of OSEC

The bare copper collector exterior and radiator became heavily oxidized at the higher collector temperatures, but not enough to cause failure of the envelope or otherwise interfere with operation. Nickel or chromium plating can be used to suppress such oxidation, however.

In view of the observed typical diode operation, it is concluded that no major limitations prevent the use of off-the-shelf componets as experimental cesium converter envelopes. Construction of a series of OSEC test models, therefore, has been initiated.

Converter Production (L.L. Begg) - The converter production effort during this period has concentrated on refining the standard converter design for use in the structured electrode series of tests. As shown in Fig. 3 a high purity alumina guard sleeve surrounding the collector has been added. This will minimize the effect of extraneous discharges at low pressures which were observed in tests of SC-2. The collector has been redesigned to include an inserted heater. This should provide improved collector temperature control, another weakness of the SC-2 design. Both SC-1 and SC-2 operated with cesium stills attached to the converter test stand. SC-3 will operate in a static vacuum with a pinch-off copper cesium reservoir.

To better meet the converter production schedule, a second outgassing station was built. It permits full bulk degassing of all converter components at a temperature of 200°C above those which will be experienced during testing. A cesium distillation oven was fabricated which permits final outgassing of the converter assembly immediately prior to cesium distillation.

A new insulator seal incorporating a bellows was designed. The use of this seal will permit adjustments in the interelectrode gap, a feature not possible with the current rigid seals. The first of the new seals should be available for use in SC-6.

An inventory of standard converter parts has been fabricated to support the converter production effort. Assembly and processing of the first structured collector converter, SC-4, was begun.

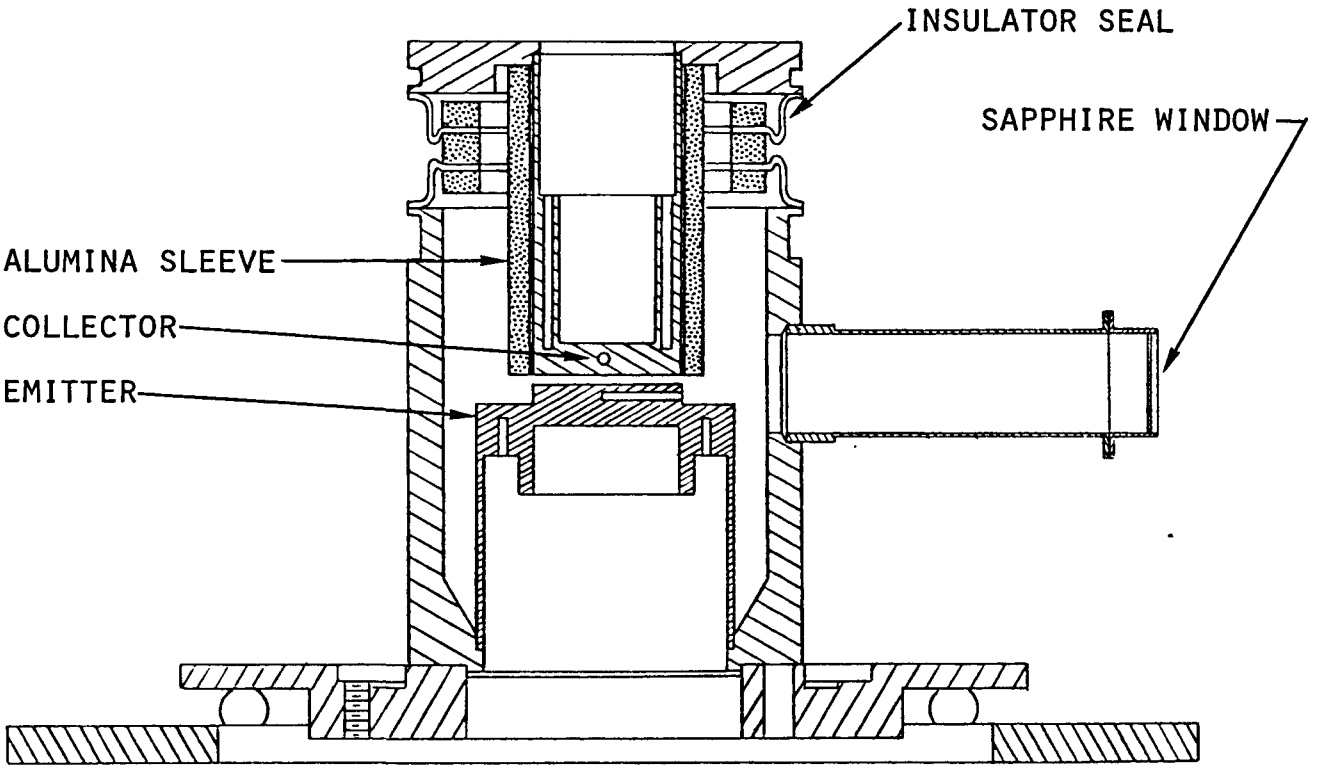

Fig. 3 SC-3 Configuration

Task 5 - Advanced Converter Development (L.L. Begg)

This task has concentrated on repairing ZEPO and preparing the high current converter test facility for the next test.

The first ZEPO tests were terminated because of multiple leaks in a bellows used to connect the two collector halves. A new bellows design was completed and the fabrication of the replacement bellows was begun. The new design incorporates two concentric bellows, as shown in Fig. 4. A two-convolution inner bellows will be used to isolate the interelectrode space, in place of the single-convolution bellows used previously. The weld joints for this bellows were redesigned to minimize stress in this area, the site of the earlier leaks. A second bellows surrounds the first and a vacuum will be maintained between the two. The second bellows serves two purposes; first it forms a second barrier against air leaks into the converter, and second is provides "vacuum insulation" for the first bellows, preventing cold spots and consequent cesium condensation. Provisions have been made for the possible addition of heaters and thermocouples in the space between the two bellows.

The initial cleaning steps were taken to recondition the converters electrode surfaces. Four holes were drilled and tapped through the welds at each end of the converter. The four igniter taps were also removed. These orifices were then used to continually flush the converter with hot soapy water over a three day period. Solvent and dilute acid cleaning steps will begin after all converter machining is complete.

Task 3000 - Basic Experimental Investigation of Advanced Operating Modes (E.J. Britt, G.L. Hatch, and L.K. Hansen)

An analytical model of a converter with spatially uniform ion generation was developed earlier as part of this program. Volt-ampere curves calculated with this model have been compared with experimental data from an argon plasmatron in previous reports. Despite the fact that ion production in the plasmatron is distinctly non-uniform (a single wire ring is used as the ionizer electrode), semi-quantitative agreement between experimental and calculated I-V curves can be obtained by treating total ion production in the gap as a parameter which can be varied with pressure

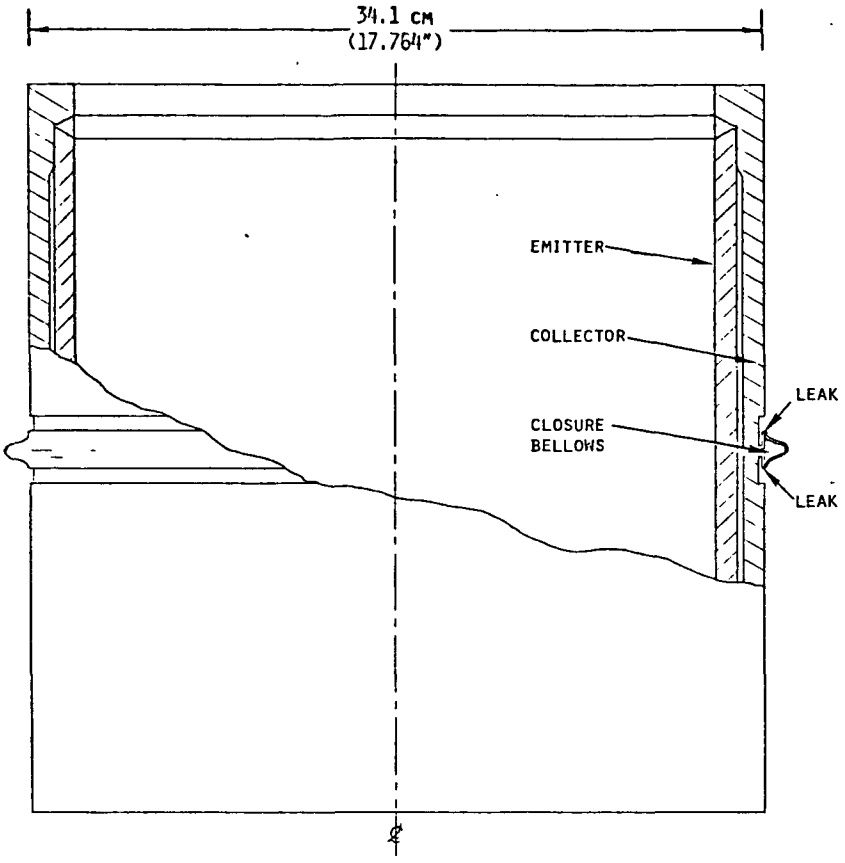

Fig. 4A Original ZEPO Design Showing Leak Location in Bellows

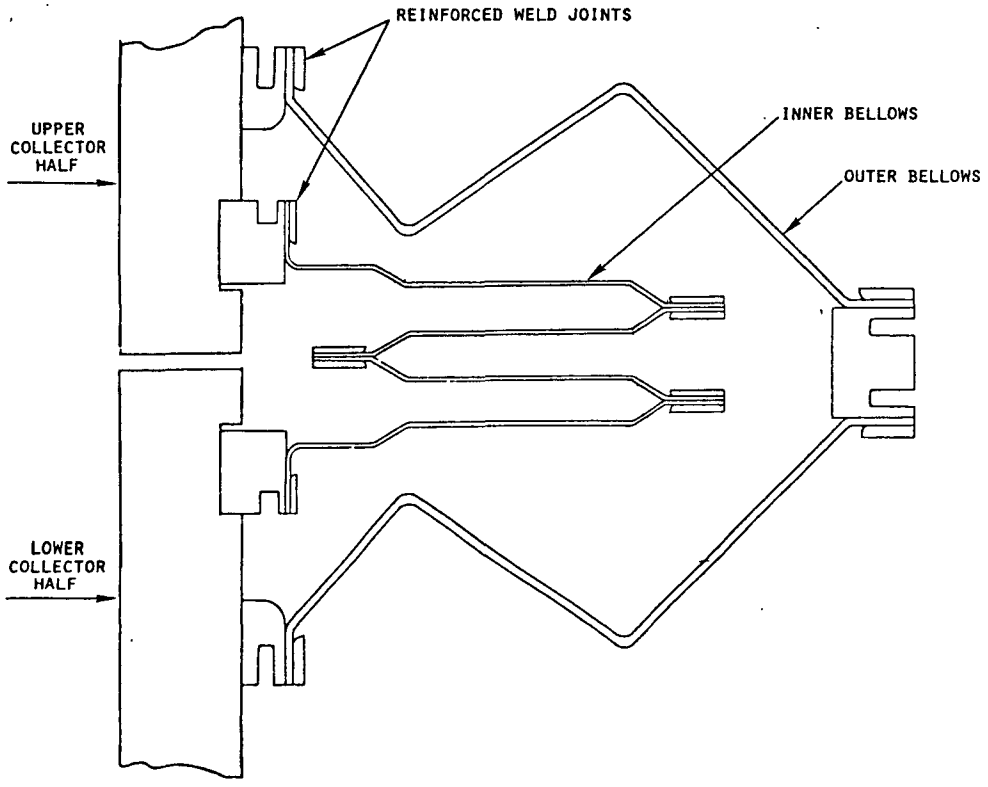

Fig. 4B Redesigned Bellows Configuration

and emitter temperature. The total ion production is designated by Sd, where S is the uniform volumetric source strength (cm^{-3} - sec^{-1}), and d is the interelectrode distance (cm).

Experimentally, a pressure family of I-V curves was taken at a fixed value of auxiliary ionizer current. This was then repeated for different emitter temperatures. In order to achieve a fit between the observed I-V families and calculated curves, the value of Sd must be varied so that it first increases with pressure to a maximum value and then drops off at higher pressures. This fit, reported first in August, is shown in Fig. 5. The theoretical value of Sd is not changed as function of the converter current or voltage, since the electrons from the ionizer are injected at ~40 volts, which is much larger than other potentials (≤ 2 volts) in the system. However, the actual ion production in the plasmatron probably varies with the plasma density (and, hence current densities). To achieve a good fit between the calculated and measured I-V characteristics requires the use of a temperature dependent Sd in the calculations. This variation of Sd with emitter temperature is not understood at present. A model which successfully describes the pressure variation of Sd is outlined below.

In a one dimensional slab geometry the ionizer wire is treated as a source plane for high energy electrons as shown in Fig. 6. The electrons for the wire are accelerated to high energy (~40 volts) by the ionizer sheath and then enter the plasma where they produce ions by collisions or are lost from the high energy group by striking the walls and relaxing in energy by electron - electron interactions. Conservation of the high energy electron group can be expressed as:

$$\frac{\partial n}{\partial t} = D \nabla^2 n - n_a \sigma_a v n - n/\tau_{ee}. \qquad (1)$$

where
- n = density of high energy electrons (cm^{-3})
- D = diffusion coefficient for the high energy electron (cm^2/sec)
- n_a = density of atoms in the gap region (cm^{-3})
- σ_a = is the atomic collision cross section for all electron interactions except elastic scattering

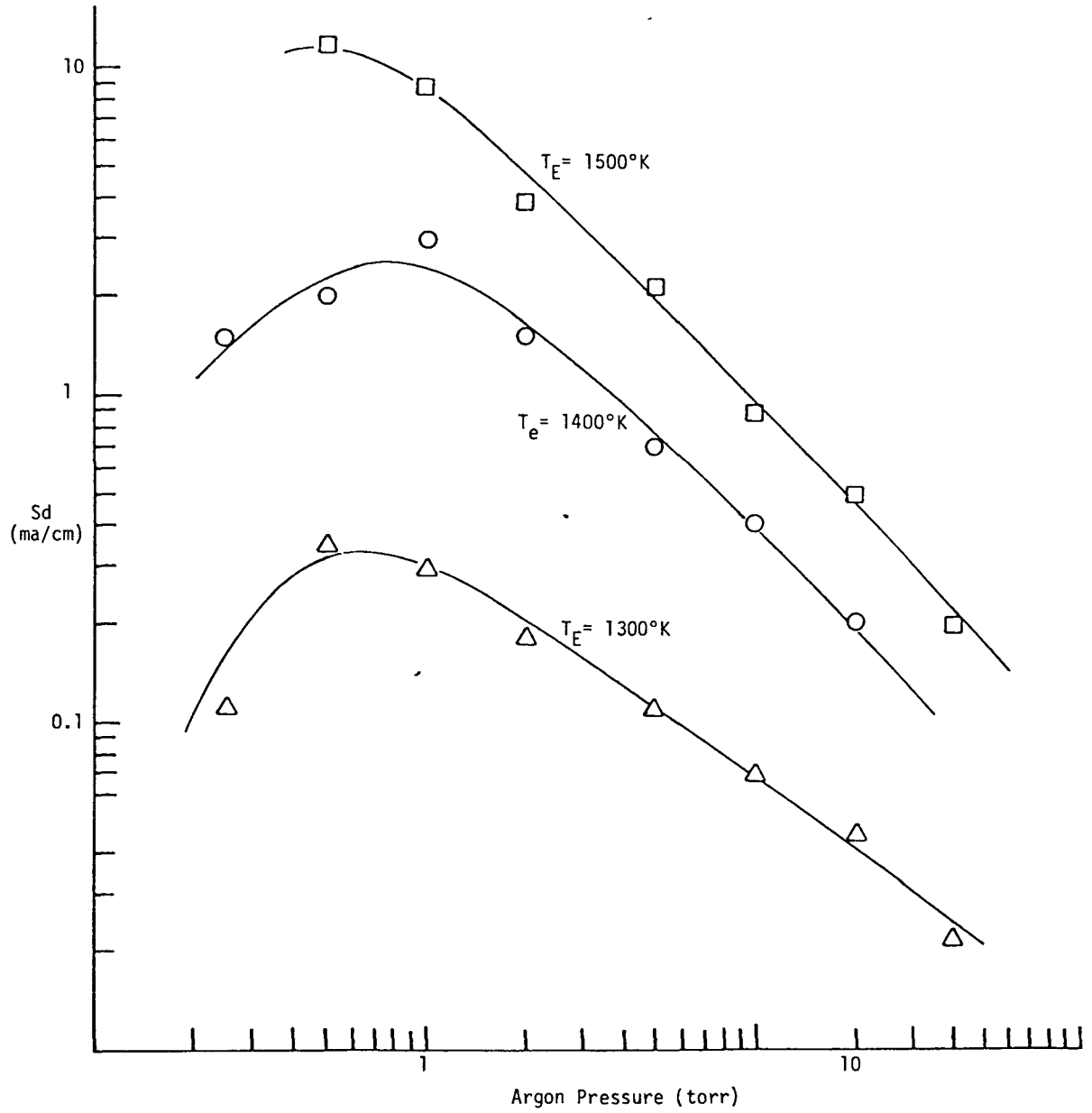

Fig. 5 Ion Source Strength Sd vs. Argon Pressure

v = is the electron-atom average relative speed (cm/sec)

τ_{ee} = the relaxation time for electrons in the plasma by coulomb interaction (sec^{-1})

At steady state

$$\frac{\partial n}{\partial t} = \nabla^2 n - \frac{n}{L^2} = 0, \tag{2}$$

where

$$\frac{1}{L^2} = \frac{n_a \sigma_a v + 1/\tau_{ee}}{D_a} .$$

The density of high energy electrons can be found by solving Eq. (7) with appropriate boundary conditions to yield

$$n(x) = \frac{I_o}{D\,[1 + \exp(-d/L)]} \left\{ \exp\left[-\frac{x}{L}\right] - \exp\left[-\frac{(d-x)}{L}\right] \right\} \tag{3}$$

where I_o denotes 1/2 I_{aux} (one half of the auxiliary current is assumed to go each way from the source plane).

The ion production rate is written as a spatially dependent source due to collisions with the high energy electrons:

$$S(x) = N_a \sigma_i \, v \, n(x) \tag{4}$$

where σ_i = cross section for ionization (cm^{-2})

At low pressure, the high energy electrons travel farther into the volume before making ionizing collisions and the ion source spreads out in the interelectrode space. However as the pressure is increased the mean free path decreases and the ion production becomes more localized around the ionizer wire. It is believed that all ions created in a narrow region near the ionizer plane was lost either by returning to the ionizer electrode or by recombination in the local dense plasma. This is reasonable since the large sheath voltage of the ionizer forms a potential well

which confines any ions in the near vicinity of the ionizer and drives them toward the ionizer. The distance within which a newly created ion is lost is designated by $\Delta/2$ (see Fig. 6). The value of $\Delta/2$ can be estimated by assuming that the potential well for ions falls off as e^{-x/L_D}, where L_D is the Debye length. The maximum depth of the well is the bias voltage of the ionizer (~ 40 volts). All ions are trapped in the region where the depth of the potential weld is greater than the thermal energy of an ion, kT_i. Thus the value of $\Delta/2$ is determined by

$$40 \exp\left(-\frac{\Delta}{2L_D}\right) \geq kT_i. \tag{5}$$

Since $kT_i \approx 0.1$ eV, $\Delta/2 \approx 5$ or 6 Debye lengths.

The total ion production in the gap is found by

$$Sd = 2\int_0^{d/2} S(x)\, dx - 2\int_0^{\Delta/2} S(x)\, dx \tag{6}$$

Evaluating the integral in Eq. (6) gives

$$Sd = \frac{2n_a\sigma_i I_o}{N_a\sigma_a + 1/v\tau_{ee}}\left[\frac{\cosh[-(d-\Delta)/2L] - 1}{\cosh[d/2L]}\right] \tag{7}$$

The expression for Sd in Eq. (7) has the correct behavior with pressure to fit the experimental I-V curves. However. Eq. (7) does not contain a dependence on emitter temperature. An indirect effect of emitter temperature is that higher current densities require larger values of plasma density and this reduce τ_{ee}. However the expected variation of τ_{ee} is not sufficient to reconcile the observed behavior with changing T_E.

The variation of Sd with emitter temperature needed to fit the data may be an artificial effect, possibly due to the use of improper boundary conditions for the calculations. As mentioned in previous reports, the calculational model can sometimes behave as though the maximum saturation current is about twice the Richardson's current from the emitter. This occurs when calculating low pressure cases with a small ion retaining sheath on the emitter side and large ion retaining sheath on the collector side, as shown in Fig. 7. The anomalously large saturation current which is

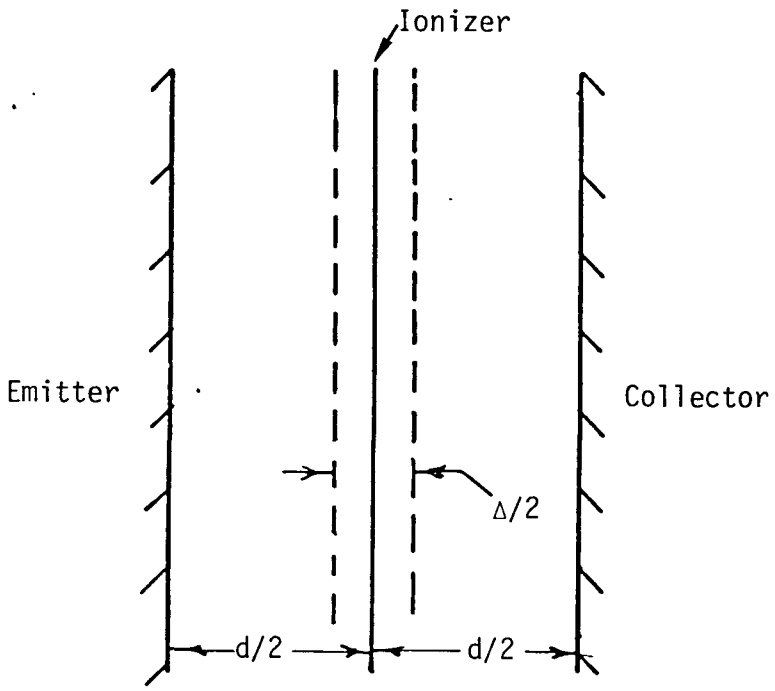

Figure 6

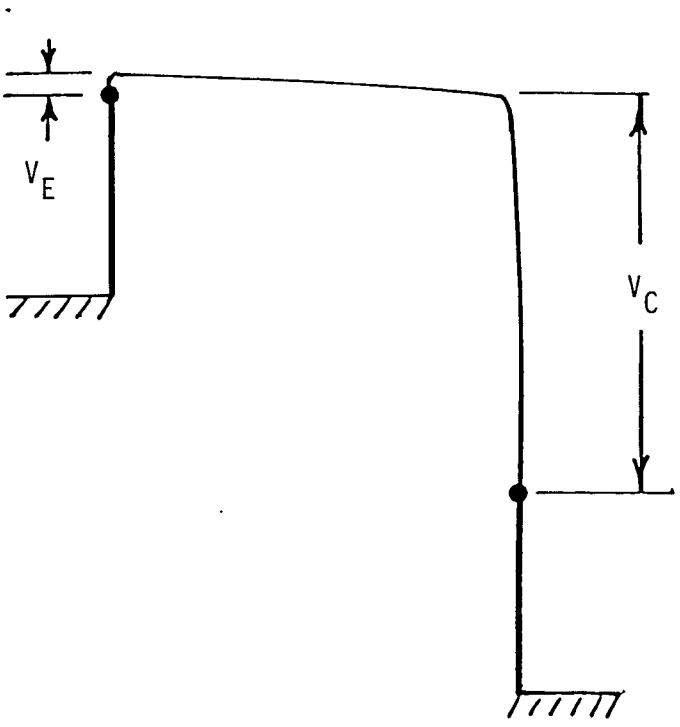

Figure 7

found under these conditions has been traced to the boundary condition for electrons at the emitter. Diffusion type boundary conditions have been used; i.e.,

$$J = J_s \exp\left(-\frac{V_E}{kT_E}\right) - \frac{en_E v_e}{4} + \frac{J}{2} \tag{8}$$

where J_S = Richardson's current density from the emitter (amps/cm^2)
V_E = height of the emitter sheath (volts)
n_E = plasma density at the emitter edge (cm^{-3})
J = net electron current density (amp/cm^2)

If V_E is small, Eq. (8) can be written as

$$J \approx 2J_S - \frac{en_E v_e}{2} \tag{9}$$

which shows that the current density can approach $2J_S$ if n_E becomes small. When the collector sheath is large enough to retain all of the ions (near saturation conditions) and the emitter sheath is small, the plasma is lost by diffusion only at the emitter and n_E is depleted. This leads to the non-physical large current.

The factor of 2 error at low values of n_e results from the use of only the first derivative term in a Taylor series expansion of the particle flux near a non-returning boundary (Refs. 1 and 2). This approximation occurs in the last term in Eq. (8). The contribution from other terms in the expansion can be neglected only if $\partial(n\vec{v})/\partial x$ is negligible over a distance of 2 to 3 mean free paths. At low pressures and/or near saturation current, these conditions are violated and hence this boundary condition leads to an error. The correct treatment of the boundary condition would require a higher order series expansion for the particle flux and its derivatives; but this introduces additional complexity in the mathematics. It has been suggested (Ref. 3) that an alternative approach is to neglect the last term in boundary conditions such as Eq. (8). The rationale for this is that when the term can be justified by a slowly varying derivative in the flux, it makes only a small change in the computed current. When the term makes an important contribution it is under conditions where it is not justified and can lead to non-physical results.

Following the suggestions described above, the boundary conditions have been changed for the uniform ion source model. The algebra for the new formulation has been developed to calculate I-V curves and a new computer program reflecting these changes is being prepared. It's hoped that I-V curves calculated with the new boundary conditions will fit the experimental data without requiring a variation of Sd with T_E.

References

1. Glastone, S. and Edlund, M.C., The Elements of Nuclear Reactor Theory, D. Van Nostrand Company, Inc., Princeton, N.J., 1962, pp. 93-100.

2. Lamarsh, J.R., Introduction to Nuclear Reactor Theory, Addition-Wesley, Reading, Maryland, 1966, pp. 125-140.

3. Prof. Harvey Lam, Princeton, University (Private Communication).